

High-Throughput Screens for Postgenomics: Studies of Protein Crystallization Using Microsystems Technology

G. Juárez-Martínez,^{†,‡} P. Steinmann,[†] A. W. Roszak,[‡] N. W. Isaacs,[‡] and J. M. Cooper^{*,†}

Department of Electronics, Rankine Building, University of Glasgow, Glasgow G12 8LT, U.K. and Department of Chemistry, Joseph Black Building, University of Glasgow, Glasgow G12 8QQ, U.K.

This paper describes the fabrication of a micromachined miniaturized array of chambers in a 2-mm-thick single crystal <100> silicon substrate for the combinatorial screening of the conditions required for protein crystallization screening (including both temperature and the concentration of crystallization agent). The device was fabricated using standard photolithography techniques, reactive ion etching (RIE) and anisotropic silicon wet etching to produce an array of 10 × 10 microchambers, with each element having a volume of 5 μL. A custom-built temperature controller was used to drive two peltier elements in order to maintain a temperature gradient (between 12 and 40 °C) across the device. The performance of the microsystem was illustrated by studying the crystallization of a model protein, hen egg white lysozyme. The crystals obtained were studied using X-ray diffraction at room temperature and exhibited 1.78 Å resolution. The problems of delivering a robust crystallization protocol, including issues of device fabrication, delivery of a reproducible temperature gradient, and overcoming evaporation are described.

Following significant industrial and academic activities in the field of genomics, the focus of attention has turned toward the study of proteins, with a particular interest in the relationship between the protein's primary and secondary structures and its three-dimensional form and function. This area of study, known as postgenomics, includes the areas of structural determinations using nuclear magnetic resonance NMR and protein crystallography, as well as more generally the understanding of the function of the biomolecules either in vitro or in the cell. Recently, the scope of post-genomic studies has extended toward measuring interactions between proteins and other biological or bioactive compounds, including other proteins (as receptors), oligonucleotides, and chemical compounds (such as drugs).¹

As stated, there are currently two major methods used to determine the three-dimensional structure of a given protein, namely NMR and X-ray diffraction. The advantage of NMR is that

it can resolve the three-dimensional structure of proteins (with molecular masses of ~20 KDa) in solution. In contrast, X-ray diffraction methods can resolve the three-dimensional structures of larger proteins or complexes, but the generation of crystals of high structural quality is crucial in order to obtain robust, high-resolution data.² The crystallization of such proteins is a multifactorial process that depends on the interplay of several independent parameters, including pH, temperature, protein concentration, crystallization agent concentration, and the presence and nature of impurities or additives.³

Although a number of proteins have been reported to have a temperature-dependent solubility, which can influence the quantity, size, and quality of the crystals,⁴ this parameter is still frequently overlooked in crystallization studies (particularly because there is often a heat of crystallization). Although it has been reported that temperature variations are important in finding optimal crystallization conditions,⁵ if these changes are not recorded and controlled, it is difficult to obtain reproducible results. By contrast with other crystallization parameters, temperature is not invasive and, thus, can be readily and intentionally modified and controlled once the crystallization experiment has begun. Moreover, exploring the relationship between temperature and other crystallization parameters increases the probability of finding new or optimal crystallization conditions.^{4,7}

To optimize crystallization condition for a given protein, the parameter space defined by the physicochemical variables of temperature, pH, ionic strength, and additional agents have to be explored, often requiring the use of large amounts of protein. Despite advances in molecular biology, many interesting proteins (e.g., the eukaryotic membrane-bound proteins) are still only available in limited quantities. Therefore, there is a necessity to produce low-volume crystallization reactors that use a reduced amount of material (while maintaining high protein concentration) and which can screen multiple variables, in a higher throughput format, simultaneously.⁸

- (2) Rosenberger, F. *J. Cryst. Growth* **1996**, *166*, 40–54.
- (3) Giegé, R.; Ducruix, A. Editors. *Crystallisation of nucleic acids and proteins: A practical approach*. IRL Press at Oxford University Press: Leeds, U.K., 1999.
- (4) Christopher, G. K.; Phillips, A. G.; Gray, R. J. *J. Cryst. Growth* **1998**, *191*, 820–826.
- (5) Drenth, J. *J. Cryst. Growth* **1988**, *90*, 368.
- (6) Heinrichs, W.; Heinrichs, M.; Schönert, H. *J. Cryst. Growth* **1992**, *122*, 186–193.
- (7) Hampton Research. *Crystallization Research Tools* **2001**, *11* (1), 136.

* To whom correspondence should be addressed. Fax: +(141) 330 6010. E-mail: jmcooper@elec.gla.ac.uk.

[†] Department of Electronics.

[‡] Department of Chemistry.

(1) Giegé, R.; Drenth, A.; Ducruix, A.; et al. *Prog. Cryst. Charact.* **1995**, *30*, 237–281.

A number of macroscale crystallization reactors with integrated temperature control^{6,9–15} have previously been reported. Others studies have begun to investigate the role of microfabrication and micromachining in devices that do not include an ability to control temperature.¹⁶ In a significant collaboration between NASA and Caliper, research is being aimed at investigating the control of protein crystallization in lab-on-a-chip (closed) systems, although both difficulties in removing intact crystals and the nonconventional format of the assay currently present major practical hurdles.¹⁷

Our current work, described in this paper, focuses on both the machining of microarrays of arrays for protein crystallization and the integration of an in situ temperature control unit. To demonstrate a proof of principle device, we have developed a 100-array element, each chamber having a total sample volume of 5 μL (into which protein solution and crystallization agent are diluted in equal amounts). Typically, the total amount of protein required for each array is a maximum of 250 μL (for 100 assays), although all of the technologies described can readily be further scaled while remaining compatible with standard laboratory procedures for protein crystallization. Using the current device, we have demonstrated the ability to investigate a number of variables, including pH, protein concentration, crystallization agent, and temperature (each of which can be varied independently). In the experiments that we describe, we have chosen to use the model system involving lysozyme for optimization of the system. This protein has well-defined and reproducible behavior and provides a crystallization process that is sensitive to both the concentration of the crystallization agent and the temperature.⁴

EXPERIMENTAL SECTION

Fabrication of the Microarray. The method of batch crystallization of protein requires that a solution of protein is mixed with the crystallization agent at a concentration such that supersaturation is instantaneously reached.³ To adapt this method to the crystallization of protein across many elements, an array of 10 \times 10 chambers was machined into a 3-in.-diameter $\langle 100 \rangle$ single-crystal silicon wafer (2 mm thick with 100 nm of low-pressure chemical vapor deposited (LPCVD) silicon nitride on both sides).

The dimensions of the array and the choice of the materials were such that there were small temperature variations across an independent titer chamber but significant differences between adjacent chambers (due to both the different thermal conductivities of silicon and water and convection currents in the chamber). The process of array fabrication is outlined as a schematic diagram, Figure 1. A layer of positive photoresist (S1818 from Microposit) was spun onto one side of the wafer at 1000 rpm. The template for the microchamber array, with each chamber

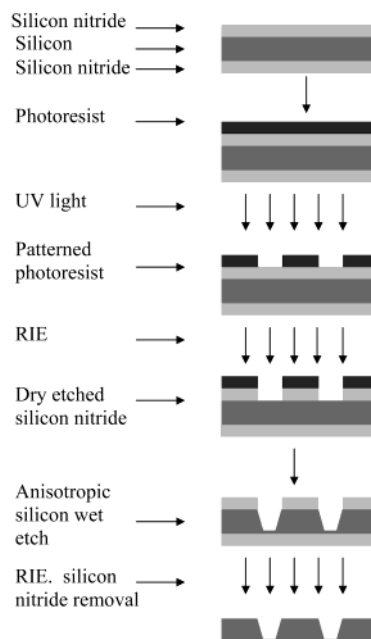


Figure 1. Schematic diagram of the fabrication process of the crystallization device.

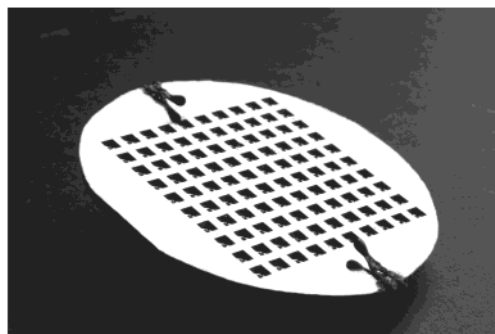


Figure 2. Photograph of the crystallization array in which each individual chamber has dimensions of 3 (W) \times 3 (L) \times 1.1 mm (D) and a separation of 2 mm.

having a footprint of 3 \times 3 mm, was defined in the photoresist using UV exposure through a corresponding photomask. The pattern was subsequently transferred into the Si_3N_4 layer by development of the photoresist (to provide a masking layer), followed by a reactive ion etch using an Oxford Plasma RIE-80 with a C_2F_6 etch, a flow meter reading of 80%, corrected flow 20 sccm, and an RF power of 100 W. The wafer was then wet-etched using a 40% aqueous solution (v/v) potassium hydroxide (Micro Image Technology Ltd. 215-181-3) to a final depth of 1.1 mm. Care was taken during the process of silicon micromachining to control the temperature of the wet-etch bath in order to ensure uniform and reproducible depths to each of the chambers. After microchamber formation, the remaining Si_3N_4 on both sides of the wafer was finally removed using the same RIE procedure. A photograph of the array is shown in Figure 2.

The Microarray System. A schematic representation of the experimental setup of the microarray and temperature controller is shown in Figure 3. Temperature control was achieved by a simple feedback system incorporating thermistors, peltier elements, and a two-channel proportional controller built in-house. To assess the temperature stability of the system, the thermistor

- (8) Chayen, N. E. *Structure* **1997**, *5*, 10, 1269–1274.
 (9) Lorber, B.; Giegé, R. *J. Cryst. Growth* **1992**, *122*, 168–175.
 (10) De Mattei, R. C.; Feigelson, R. S. *J. Cryst. Growth* **1993**, *128*, 1225–1231.
 (11) Lorber, B.; Giegé, R. *J. Cryst. Growth* **1996**, *168*, 204–215.
 (12) Carter, D. C.; Wright, B.; Miller, T.; et al. *J. Cryst. Growth* **1999**, *196*, 602–609.
 (13) Carter, D. C.; Wright, B.; Miller, T. *J. Cryst. Growth* **1999**, *196*, 610–622.
 (14) Luft, J. R.; Rak, D. M.; De Titta, G. T. *J. Cryst. Growth* **1999**, *196*, 447–449.
 (15) Pletser, V.; Stapelmann, J.; Potthast, L.; et al. *J. Cryst. Growth* **1999**, *196*, 638–648.
 (16) Sanjoh, A.; Tsukihara, T. *J. Cryst. Growth* **1999**, *196*, 691–702.
 (17) Press Releases. Calipertech. 23 July 2001. <http://www.calipertech.com/company/pr/pr072301.html>.

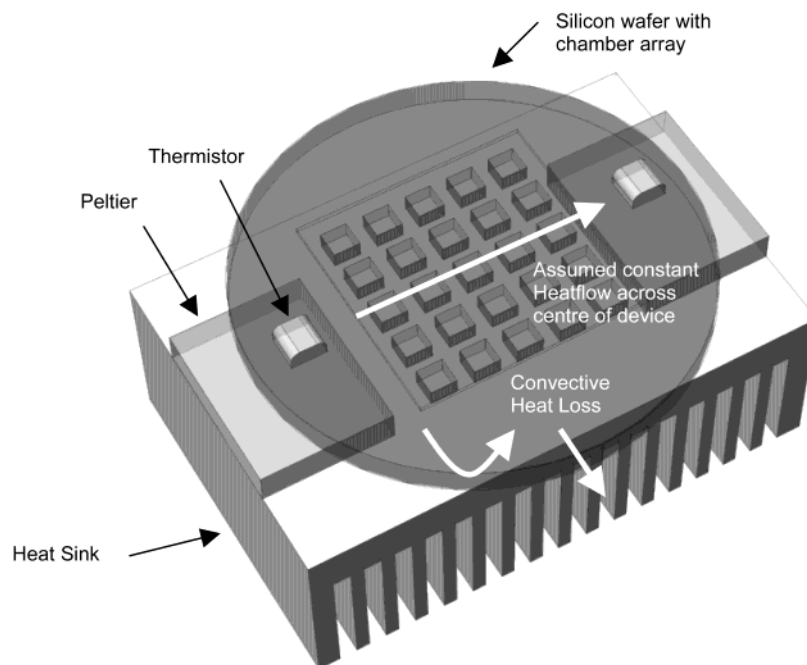


Figure 3. Schematic representation of the experimental setup. For clarity, a 5×5 array of chambers is shown, whereas crystallization experiments were generally carried out using a 10×10 array. The figure also shows the directions of the assumed heat flow. The silicon wafer has a diameter of 3 in. and a thickness of 2 mm. Note: The silicon wafer and the heatsink are not in contact (there is an air gap between them). The heatsink is required for efficient operation of the peltier element.

signals were logged using a data acquisition system. Analysis of these data confirmed a long-term stability of ± 0.1 °C between 0 °C and 50 °C. The time to reach equilibrium was dependent upon the ambient environment, which was maintained locally at 27 °C with minimal airflow. Of particular interest in studying the design of the array is the steady state thermal behavior of the system. To a first approximation, modeling has been carried out using the one-dimensional equation of heat flow per unit area, Q , according to

$$Q = -K \frac{dT}{dx} \quad (1)$$

where K is the thermal conductivity.

Because both sides of the device are held at a fixed temperature, it is reasonable to assume that the heat flow across the bulk of the device is constant, yielding the simple linear solution

$$T = C - \frac{Q}{K}x \quad (2)$$

where C is a constant of integration subject to ambient conditions. Heat losses will occur at the perimeter of the device, which in a regulated environment will add a corrective constant term to the value of Q , in this case x . As expected, at the edges of the wafer, the gradient is less uniform, and in practice, measurements are best made in the center of the array. In a working device, such deviations could be readily compensated for either in the physical design or experimentally.

Crystallization Reagents. Hen egg white lysozyme was from Fluka (Rieden-de Haën); sodium acetate (S-9513) and sodium nitrate (22,134-1) were purchased from Sigma Chemical Co.

Protein cleaning solution was from Protein Solutions Inc. All other reagents, unless stated, were from Aldrich. Where appropriate, all of the solutions were prepared with deionized water from a Millipore Elix 10 System and were subsequently filtered using a $0.22\text{-}\mu\text{m}$ Whatman filter.

Crystallization Experiments. The samples were prepared in Eppendorf tubes by adding equal volumes of a solution of lysozyme (at a final concentration of 30 mg mL^{-1}) and the crystallization agent, sodium nitrate (with a range of final concentrations varying in a stepwise manner between 33 and 800 mM). All solutions were equilibrated in acetate buffer, pH 4.5. Once the final crystallization solutions were made, the crystallization arrays were filled with $5 \mu\text{L}$ of these solutions using a micropipet, in a temperature- and humidity-controlled environment. To minimize the effect of the evaporation, sealing of the device was performed immediately using the industry-standard Crystal Clear sealing tape from Hampton Research Co. Alternative strategies to overcome evaporation, including the use of polymers, such as moulded poly(dimethylsiloxane) overlayers, were tested, although the self-sealing tape provided the most convenient and robust method to mitigate against evaporation and to enable the recovery of the crystals at the end of the experiment.

The peltier elements were maintained at 12 and 40 °C, respectively, and the temperature in each microchamber was measured using a precision calibrated thermistor (RS products, U.K.). The crystallization experiment was stopped and examined for crystals after 12 days.

RESULTS AND DISCUSSION

The use of silicon as a substrate for the protein crystallization array has some clear advantages, including the fact that these are well-established procedures for its micromachining, enabling

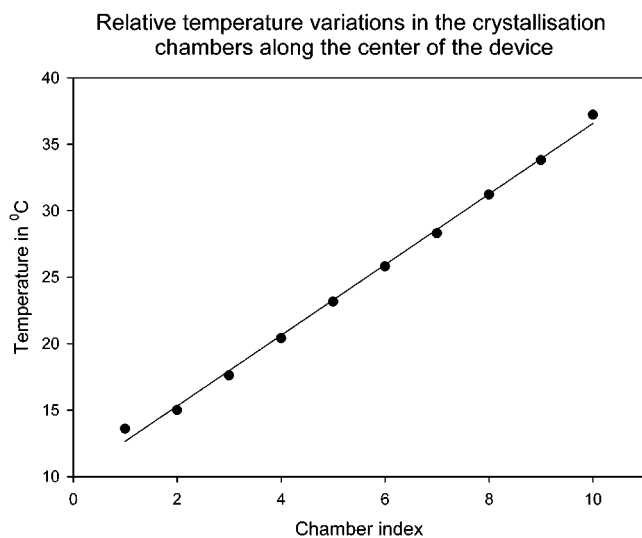


Figure 4. Temperature variation along the center of the device. The spacing (center to center) of the chambers is 5 mm.

a robust and reproducible fabrication process. Silicon has a thermal conductivity of $K \sim 150 \text{ W m}^{-1} \text{ K}^{-1}$ at 20 °C, which makes it a good substrate for devices that require a rapid and efficient heat transfer.¹⁷ The use of silicon does, however, present some disadvantages, namely the high cost of nonstandard wafers and the lack of optical transparency (which makes observation of the protein crystals difficult without the addition of a dye). However, the device can be readily cleaned and reused, although care must be taken in the cleaning protocol to avoid contamination between proteins (commercial solutions for removing proteins are readily available).

Miniaturization of the array, and the associated peltier elements, requires less power for heating and cooling the sample. The dimensions of the chambers described in this paper are limited not by the fabrication methods used, but rather by considerations of the user interface in a standard laboratory (where robots may not be available).¹⁹ In contrast to other devices for thermal manipulation of fluids, such as those used for polymerase chain reaction (where volumes may be $<1 \mu\text{L}$, but reaction times are fast), protein crystallization experiments may take several days or months. As a result, one of the major problems was the sealing of the crystallization chambers²⁰ (to prevent evaporation). This led us to use a larger volume that might be the case at the limits of miniaturization. Indeed, future experiments currently underway and including those involving vapor diffusion and counter diffusion crystallization methods, can more readily be formatted in closed microsystems and may be more amenable to further reductions in size (for example, using “industry-standard” formats of array element densities, such as 1536 or 3456 footprints).

The temperature of individual chambers was measured using thermistors, Figure 4, and showed a close correlation with the model proposed in eqs 1 and 2. As shown in Figure 5, there was a linear gradient across the bulk of the microarray, although as

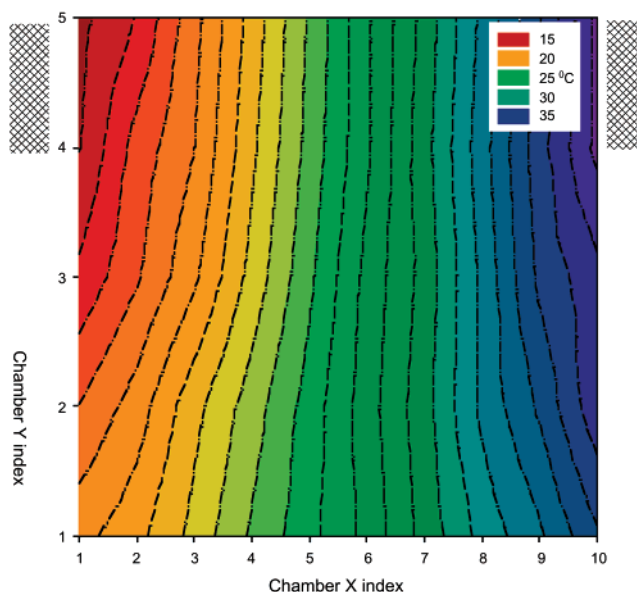


Figure 5. 2D temperature distribution measured across one-half of the device. The crosshatched boxes indicate the approximate relative positions of the peltier elements.

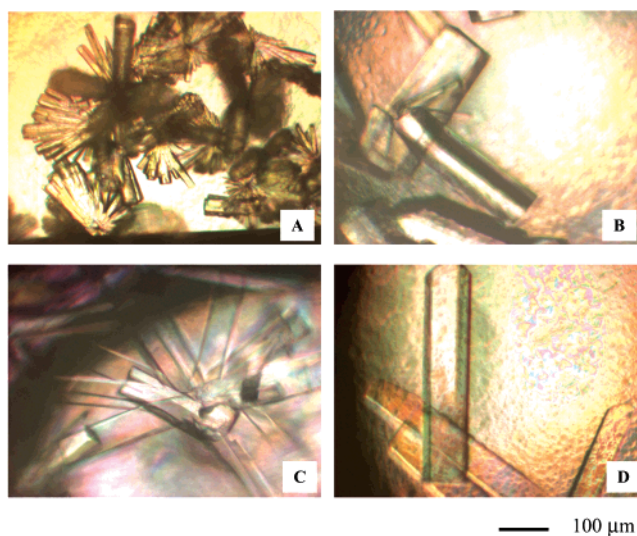


Figure 6. Protein crystals obtained with the crystallization device using crystallization conditions in which the protein concentration was 30 mg mL^{-1} , crystallization agent concentration (NaNO_3) was 0.4M, and the pH was 4.50. A–D are images of chambers at the different temperatures where the protein crystals were grown: 13.6, 17.6, 23.1, and 25.8 °C, respectively.

expected, there is a reduced heat loss from those chambers situated close to the peltiers. Initial crystallization experiments involving lysozyme concerned the use of sodium nitrate as a crystallization agent, making this protein more sensitive to the temperature changes.²¹ In Figure 6, clear morphological differences can be observed as a function of the temperature gradient across the device at constant concentration of the crystallization. Rodlike clusters appear at lower temperatures (Figure 6a), which gradually transform to single crystals at higher temperatures (Figure 6b–d). These results agree closely with complementary data previously published²¹ based upon a single chamber protein

(18) Daniel, J. H.; Iqbal, S.; Millington, R. B.; et al. *Sens. Actuators* **1998**, *A71*, 81–88.

(19) Wilding, P.; Kricka, L. J. *TIBTECH* **1999**, *17*, 465–468.

(20) Mueller, U.; Nyarsik, L.; Horn M.; et al. *J. Biotechnology* **2001**, *85*, 7–14.

(21) Jones, W. F.; Wiencek, J. M.; Darcy, P. A. *J. Cryst. Growth* **2001**, *232*, 221–228.

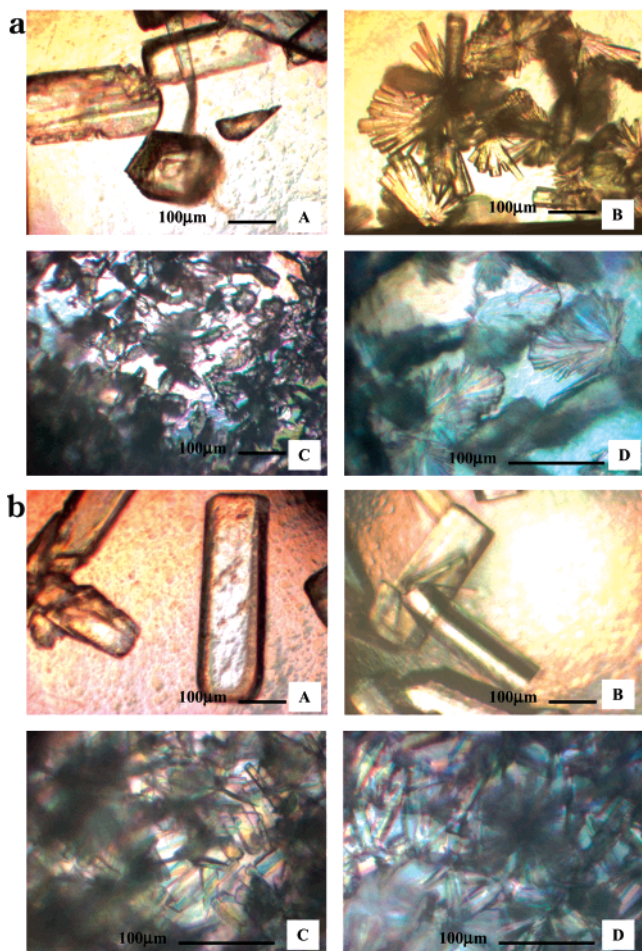


Figure 7. (a) Micrographs of the protein crystals. The crystals were grown at 14.4 ± 0.8 °C using different concentrations of crystallization agent (NaNO_3): (A) 0.30, (B) 0.40, (C) 0.50, and (D) 0.60 M. Note that D was photographed at higher magnification for a clearer observation of the crystals (which were extremely small). (b) Micrographs of the protein crystals. The crystals were grown at 18.2 ± 0.6 °C using different concentrations of crystallization agent (NaNO_3): (A) 0.30, (B) 0.40, (C) 0.50, and (D) 0.60 M. Note that parts C and D were photographed at higher magnification for a clearer observation of the crystals.

crystallization assay, with integrated thermal control. In contrast to our microsystem, this single device²¹ provides discrete data points, rather than a continuum of information concerning the change in the solubility of the sample associated with a change in temperature.

Experiments were conducted over 12 days, and the results indicate that at low concentrations of sodium nitrate (33–200 mM), there was no crystallization, a fact that is explained by the high solubility of the protein under these conditions (data not shown). As the concentrations of crystallization agent are increased between 300 and 600 mM, crystals of decreasing size are formed (see Figure 7a,b). The influence of the crystallization agent and temperature on the size of the crystals is presented in Table 1. For clarity of presentation, only length is tabulated, similar trends exist for both crystal width and depth. At the highest concentrations of sodium nitrate studied (800 mM), an amorphous semicrystalline precipitate was formed.

To verify diffraction quality of the crystals obtained with this device, a crystal from the condition shown in Figure 7d was

Table 1. Mean Length of Two Sets of Crystals for Different Concentrations of the Crystallization Agent NaNO_3 ^a

concn NaNO_3 / M	mean crystal length/ μm^b	mean crystal length/ μm^c
0.30	233	408
0.40	125	292
0.50	40	79
0.60	41	amorphous

^a 0.30–0.60 M. ^b Crystals grown at 14.4 ± 0.8 °C. ^c Crystals grown at 18.2 ± 0.6 °C.

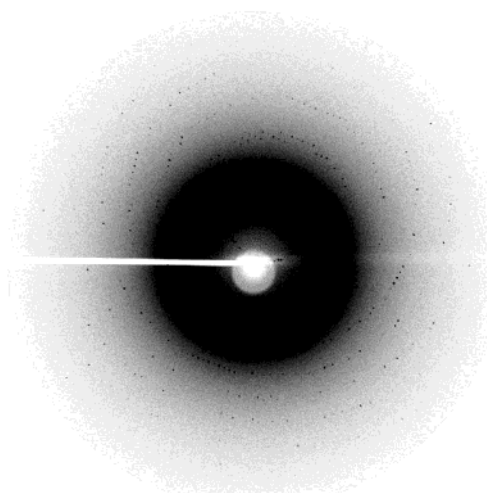


Figure 8. Example of diffraction pattern from our lysozyme crystal with the resolution of 1.78 Å at the edge of the detector.

chosen for X-ray diffraction analysis. The crystals obtained were from the monoclinic system, space group $P2_1$, with the cell dimensions $a = 28.010$ Å, $b = 62.947$ Å, $c = 60.512$ Å, and $\beta = 90.698$ deg. Diffraction data were collected at room temperature, for the crystal mounted in the capillary, using an in-house X-ray source (Nonius FR591 Rotating Anode Generator and an image plate detector MacScience DIP2000).

Figure 8 shows an example of the diffraction pattern from our lysozyme crystal with the resolution of 1.78 Å at the edge of the detector. A total of 180 frames were collected (1° , 20-min exposure/image), which produced 20 163 unique reflections. The average I/s for all data was 7.8; the average redundancy, 3.6; the overall completeness, 99.7%; and R_{merge} 8.3%. Processing of the data was performed using the programs from the HKL suite of programs. These data demonstrate that the crystals produced with this device are suitable for high-quality X-ray diffraction analysis.

CONCLUSIONS

A micromachined array of chambers for protein crystallization has been presented that includes a simple method of establishing a temperature gradient across the array of protein crystallization chambers. In addition to discussing the relative merits of the materials system (in the context of cost, reproducibility, optica, and thermal properties) a simple argument based on physical heat flow is also presented and is shown to correspond closely with the measured temperature distribution. The behavior of the system has been demonstrated using the crystallization of a model

protein, thereby demonstrating the effect of temperature and the concentration of crystallization agent.

Further work currently in progress concerns the fabrication of microarrays for vapor diffusion and counterdiffusion crystallization methods, both of which will utilize a similar temperature gradient across closed system devices. In the future, the ability to screen the conditions of crystallization and define the optimal parameter space will increase the probability of finding new crystallization conditions. Such devices will be particularly valuable in optimizing the conditions for intractable biological systems, including those such as membrane-bound proteins that are not only difficult to purify in large amounts, but also are difficult to crystallize (requiring agents and detergents).

Notwithstanding the problem of evaporation, reduction in the size and increasing numbers of the crystallization chambers will be possible in future devices, providing a route for high-throughput screening of crystallization conditions for postgenomics. In this

report, the chamber size, geometry, and spacing, as well as the choice of materials will also be critical in determining final array densities. Inevitably, robotic systems for loading the samples and for monitoring the growth of the protein crystals will be of increasing importance in such systems and will drive.

ACKNOWLEDGMENT

The authors acknowledge Philip Davis, Marlow Technologies, for his advice regarding thermal engineering and Dr. Andrew Glidle for his help. G.J.-M. acknowledges financial support from CONACyT-México, scholarship-loan, Register No. 133360.

Received for review December 11, 2001. Accepted April 16, 2002.

AC0112519